Defense Technical Information Center
Compilation Part Notice

ADP011200

TITLE: Nanoscale Decoration of Electrode Surfaces with an STM

DISTRIBUTION: Approved for public release, distribution unlimited

This paper is part of the following report:

TITLE: Internal Workshop on Interfacially Controlled Functional
Materials: Electrical and Chemical Properties Held in Schloss Ringberg,
Germany on March 8-13, 1998

To order the complete compilation report, use: ADA397655

The component part is provided here to allow users access to individually authored sections
of proceedings, annals, symposia, etc. However, the component should be considered within
the context of the overall compilation report and not as a stand-alone technical report.

The following component part numbers comprise the compilation report:
ADP011194 thru ADP011211

Nanoscale decoration of electrode surfaces with an STM

D.M. Kolb*, G.E. Engelmann, J.C. Ziegler

Department of Electrochemistry, University of Ulm, 89069 Ulm, Germany

Abstract

The tip of a scanning tunnelling microscope (STM) has been used to deposit nanometer-sized clusters of copper or silver on bare and thiol-covered gold electrode surfaces at predetermined positions. First, metal is deposited electrochemically onto the STM tip, then the clusters are formed by a jump-to-contact between the tip and the substrate during a short and very controlled approach of the tip towards the surface. When Ni is deposited onto the tip, the jump-to-contact occurs in the opposite direction leaving holes in the gold surface. The stability of the metal clusters against anodic dissolution is discussed. Finally, it is shown how the tip approach can be used to determine tunnel barriers at the metal–electrolyte interface. © 2000 Elsevier Science B.V. All rights reserved.

1. Introduction

The past few years have witnessed the tremendous success of scanning tunnelling microscopy (STM) not only as a technique to image surfaces in real space and with atomic-scale resolution, but also as a tool for positioning single atoms and molecules on surfaces with an hitherto unprecedented precision. The tip–substrate interaction at close distances (say, of the order of an atomic diameter), which generally is a much feared problem in surface imaging as it may give rise to artefacts, has been successfully employed to manipulate single atoms or molecules with the tip. Impressive examples of this kind of nanostructuring have been given by several groups working under ultrahigh vacuum conditions (UHV) and mainly at low temperatures [1–5]; among them is Don Eigler's famous quantum corral, which consists of 48 Fe atoms arranged with the tip of an STM in a circle on a Cu(111) surface [6].

The nanostructuring of electrode surfaces, primarily of noble-metal or graphite surfaces in contact with an aqueous solution, started soon after the corresponding work in UHV, although the tip-generated entities were clearly larger than individual atoms. Structures from single atoms would not have been stable enough to survive in an electrochemical environment at room temperature. The most common approach to an electrochemical nanostructuring of surfaces was to create surface defects by the tip, which then acted as nucleation centers for the metal deposition at preselected positions [7–9]. This was

---

*Corresponding author. Tel.: + 49-731-502-5400; fax: + 49-731-502-5409.

E-mail address: dieter.kolb@chemie.uni-ulm.de (D.M. Kolb)

done by applying high-voltage pulses (1.5–6 V) for a short (μs) or ultrashort (ns) time between tip and sample that leads to the formation of holes in the surface by either mechanical contact or some sort of sputtering process. Metal deposition from solution was subsequently observed at the tip-induced defects. Quite recently, metal clusters were shown to be positioned at will on metal and semiconductor surfaces by a two-step process that involves metal deposition from solution onto the tip, followed by a burst-like dissolution and redeposition on the sample right underneath the tip [10,11]. Over the last several years our group has developed yet another technique, by which flat electrode surfaces can be decorated with small metal clusters via a tip-induced deposition that leaves the sample surfaces undamaged [12–16].

In the following, we will briefly reiterate the principles of our method and show some examples of Cu clusters on bare and thiol-covered Au(111), before results on a new system, namely Ag clusters on Au(111), are presented. Like in the case of Cu clusters, a surprisingly high stability of the small Ag clusters on gold against anodic dissolution is found. Finally it is shown what happens to a gold surface during the tip approach, if a metal with high cohesive energy like Ni has been deposited onto the tip.

2. Experimental

The experimental set-up for nanostructuring a gold surface with metal clusters has been described in previous publications [13–16]. For the sake of convenience, however, the most pertinent data are briefly repeated here. For nanodecoration and surface imaging a PicoSPM (Molecular Imaging, Tempe, USA) was used with separate control of tip and sample potential by a bipotentiostat. The tip approach, during which the transfer of metal from the tip to the substrate occurs, was enforced by applying a voltage pulse directly onto the z-piezo. Actually, tip approach as well as tip movement in x- and y-direction during nanostructuring was externally controlled by a microprocessor which makes the cluster formation and the surface decoration a fully automated process.

STM tips were made from a 0.25-mm diameter Pt/Ir (80:20) wire that was etched in a lamella of 3.4

M NaCN. The tips were coated either with Apiezon wax [17,18] or with an electrodeposition paint [19] to reduce the area in contact with the electrolyte down to about 10^{-7} cm^2. Consequently, Faradaic currents at the tip/electrolyte interface were typically below 50 pA and thus, sufficiently lower than our tunnel currents which were usually around 2 nA. All STM images were obtained in the constant-current mode. They are unfiltered, but corrected for any tilt of the sample surface.

The samples were either Au(111) films on glass or a massive Au(111) crystal. Both types of electrodes were flame-annealed at yellow heat in a H$_2$-flame [20,21] and cooled down to room temperature in a nitrogen atmosphere prior to each experiment. The ethanethiol-covered Au(111) surface was obtained by immersing the Au(111) film electrode overnight in a 1 mM ethanolic solution of ethanethiol where a so-called self-assembled monolayer (SAM) is spontaneously formed [22]. The reference electrodes were simply a Cu or a Pt wire for Cu deposition, Hg/Hg$_2$SO$_4$ for Ag deposition and a Pt wire for Ni deposition. The solutions were 0.05 M H$_2$SO$_4$ with 0.1 or 1 mM CuSO$_4$ and Ag$_2$SO$_4$ for Cu and Ag deposition, respectively, and 0.01 M H$_3$BO$_3$ + 0.2 mM HCl + 1 mM NiSO$_4$ (Watts bath) for Ni deposition, made of Merck suprapur chemicals except for CuSO$_4$, Ag$_2$SO$_4$ and NiSO$_4$, which were of p.a. quality. In the case of Cu and Ag deposition, potentials are quoted against the reversible Me/Me^{z+} potential in that solution, in the case of Ni, all potentials are quoted against SCE.

3. Results and discussion

3.1. Cu clusters on Au(111)

The proposed mechanism for the tip-induced cluster formation is sketched in Fig. 1, highlighting the two requirements that have to be fulfilled:

(i) First, metal has to be deposited onto the tip, which is achieved by simply choosing a tip potential negative of the corresponding bulk metal deposition potential.

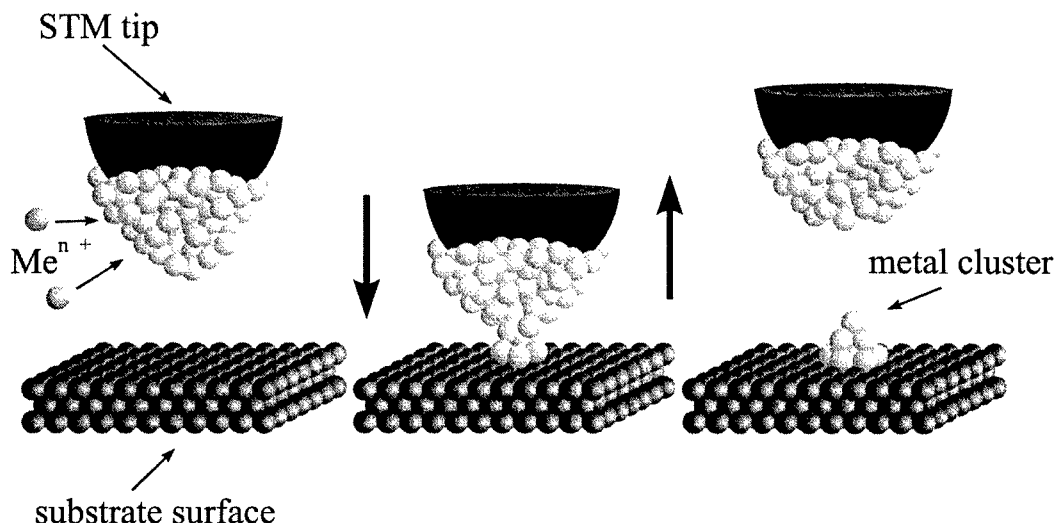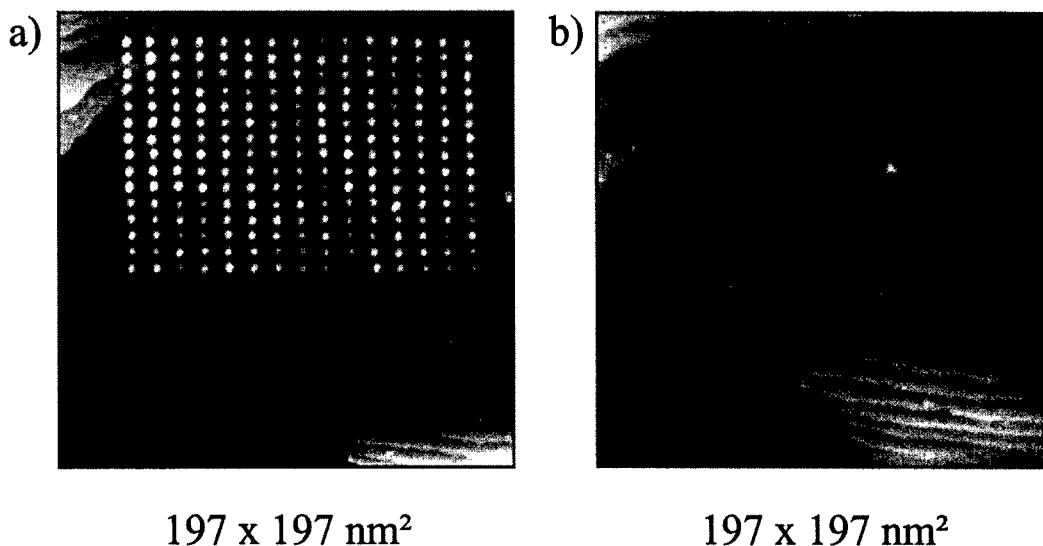(ii) Secondly, the metal-loaded tip has to approach the surface for a short period of time,

Fig. 1. Schematic diagram of the tip-induced cluster formation.

during which a so-called jump-to-contact [23,24] occurs.

The resulting connective neck breaks upon the subsequent retreat of the tip leaving a small metal cluster on the surface. We stress the point that the direction of the material transfer will depend on the cohesive energies of both sides, and for Ni and Au(111) it is opposite to the Cu case (see Section 3.4 and Ref. [24]). As has been shown before, the externally enforced tip approach allows the fast generation of Cu clusters with a remarkably uniform size distribution. In Fig. 2a an array of 225 Cu clusters is shown, all about 0.6 nm high, which was

Fig. 2. (a) STM image of an array of 225 Cu clusters on Au(111) in 0.05 M H_2SO_4 + 0.1 mM $CuSO_4$ generated by 225 voltage pulses to the z-piezo. The Cu clusters are placed on a Cu-monolayer-covered Au(111) surface due to underpotential deposition. E_{sample} = + 10 mV vs. Cu/Cu^{++}, E_{tip} = − 30 mV, I_t = 2 nA. (b) Same area, but after anodic dissolution of the Cu clusters at + 300 mV.

accomplished within 30 s. Besides the remarkably uniform cluster height, several points are noteworthy. The clusters were generated with 2-ms voltage pulses to the z-piezo with a repetition rate of 120 Hz. With a minimum pulse duration of 0.1 ms as determined in earlier experiments [25], a much higher cluster deposition rate, e.g. in the kHz range, seems feasible. Furthermore we note from Fig. 2a that monoatomic high steps of the substrate cause no problems for the preselected cluster patterning, suggesting that nanostructuring of slightly rough surfaces by our technique may still work. Despite the fabrication of many Cu clusters in quick succession (the largest array so far consisted of 10 000 Cu clusters [26]), there is no sign of depletion of Cu on the tip. The re-filling of the tip during the cluster fabrication by an on-going deposition reaction at the tip is surprisingly fast and — quite importantly — retains the high imaging quality of the tip. Hence, 'writing' and 'reading' are possible with the same tip. Anodic dissolution of the Cu clusters uncovers a perfectly flat Au(111) surface (Fig. 2b), a fact that supports our statement of an undamaged surface and that we are not dealing with tip-induced defects in the substrate. In other words, a tip-induced nanostructure can be completely erased. Finally, the stability of the Cu clusters against anodic dissolution is remarkable [11,14,27]. Studies have shown that the Cu nanoclusters are stable at $+10$ mV vs. Cu/Cu^{++} for at least 1 h and considerable 'overpotentials' of $+100$ mV and more are required to dissolve the tip-induced Cu clusters completely within minutes. Similar findings will be reported in Section 3.3 for Ag clusters on gold. The origin of this unusual electrochemical stability of the nanofabricated clusters has been explained on the basis of a quantum-size effect [27].

As mentioned before, all three spatial coordinates of the tip can be externally controlled by a microprocessor, which makes the nanodecoration of an electrode surface with metal clusters a fully-automated process, allowing even complex patterns to be made fast and reproducible. Fig. 3 shows a pattern made of about 400 Cu clusters on Au(111) with the clusters arranged in a rhombic fashion. The clusters are sitting on quite a stepped Au(111) surface, which is covered by a monolayer of Cu due to underpotential deposition (upd) at $E_{sample} = 10$ mV vs. Cu/

Cu^{2+}. Other, more complicated structures such as letters and words, have been shown in previous publications [16].

The Cu clusters presented so far were all formed directly by the jump-to-contact during tip approach. Their height can be varied within certain limits by the extent of the approach, typically within 0.3–1.2 nm (i.e. from one to about five Cu monolayers) [13–15]. In certain instances, however, somewhat larger clusters are desirable, e.g. when dealing with magnetic metals. In such a case, the tip-induced metal clusters can be used as nucleation centers to grow larger ones at predetermined positions by normal deposition from solution. In Fig. 4 a so-called $x - t$ scan is shown, where a single scan in the x-direction is repeatedly recorded ($y = $ constant) and plotted as a function of time. Thus the development of a certain structural feature with time, like the growth of an individual cluster, can be monitored in great detail. The image in Fig. 4 shows the growth of a tip-generated Cu cluster after the potential was stepped from $+10$ mV vs. Cu/Cu^{++} to -280 mV vs. Cu/Cu^{++}. It can be clearly seen that the tip-generated cluster first grows mainly laterally, before several new layers nucleate on top of the cluster. Within the time span covered in Fig. 4, a total of eight Cu monolayers is seen to nucleate and grow on the tip-induced cluster, expanding the latter to a formidable size.

3.2. Cu clusters on thiol-covered Au(111)

An important question to be addressed in the near future is the influence of a chemical surface modification on the tip–substrate interaction in general and on the jump-to-contact behaviour in particular. Self-assembled monolayers (SAM) of alkanethiols on Au(111) are among the most popular systems for surface chemical modifications, because well-ordered and stable adlayers are conveniently achieved simply by dipping the sample for a prolonged period of time in an ethanolic solution of the thiol under consideration. Since our group has recently finished an extended investigation on the structure of ethanethiol on Au(111) [22], we used this system to test whether tip-generated Cu clusters can be placed on such surfaces. Fig. 5 demonstrates that this is indeed
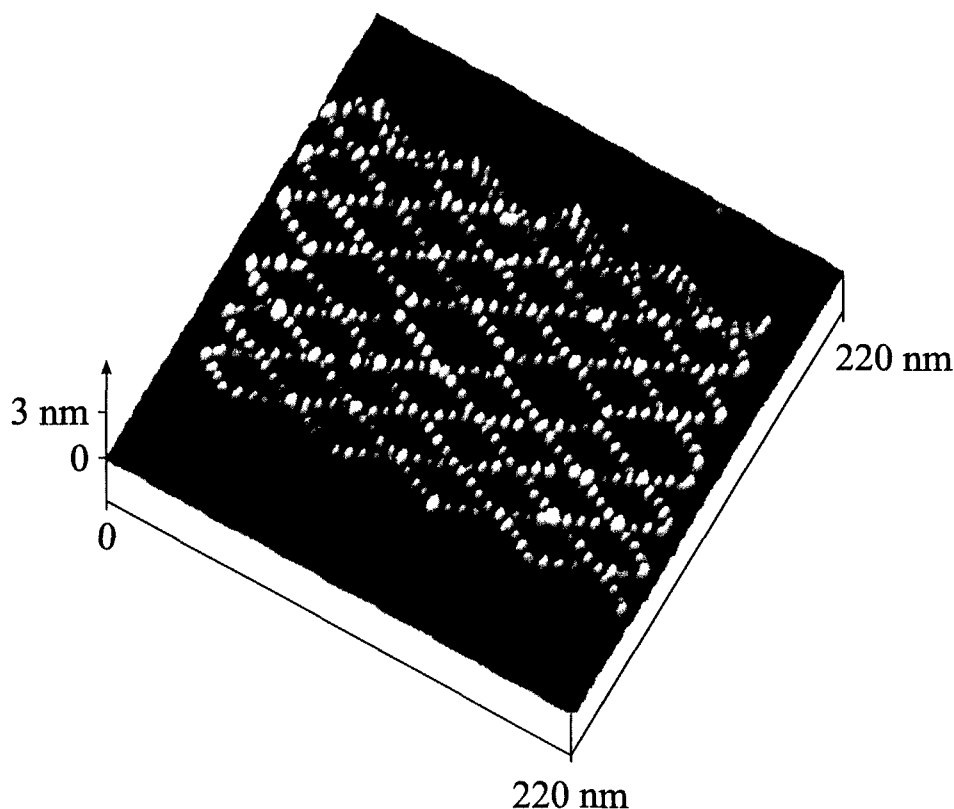
Fig. 3. STM image of about 400 Cu clusters on Au(111) in 0.05 M H_2SO_4 + 1 mM $CuSO_4$. E_{sample} = + 10 mV vs. Cu/Cu^{++}, E_{tip} = − 30 mV, I_t = 2 nA.

possible. A square array of 25 Cu clusters with heights between 0.7 and 1.1 nm was generated by 25 externally enforced tip approaches. It was recently shown in our group that at a potential of + 10 mV vs. Cu/Cu^{++} which is required to keep the Cu clusters on the surface for a longer period of time, the ethanethiol SAM is in a disordered state with small ethanethiol islands on top of it [22]. These islands are clearly seen in Fig. 5 as grey, 0.2 nm high blobs scattered all over the surface. Anodic dissolution of the Cu clusters left a Au(111) surface with an intact SAM. Because of the structural transition of the ordered SAM at about 200 mV vs. Cu/Cu^{++} into a disordered state, which prevails at potentials closer to the Cu/Cu^{++} Nernst potential, we are presently not able to characterize on a molecular level the SAM structure onto which the Cu clusters are placed. However, it is reasonable to assume that the

disordered state is less densely packed with ethanethiol molecules than the ordered state, the molecularly resolved STM images of which clearly reveal structures with a maximum coverage of about one-third monolayer. It thus appears that Cu atoms at the tip can still interact with a sufficiently large number of bare gold atoms to allow a jump-to-contact to occur.

We note in passing that very similar arrays of Cu clusters were also produced with octadecanethiol-covered Au(111) electrodes [28]. The fact that the alkane chain length apparently has no major influence on the cluster generation process seems understandable in view of the close proximity of tip and substrate: under the experimental conditions which we have chosen, the tip is ploughing through the alkane chains of the thiol monolayer rather than scanning above it.
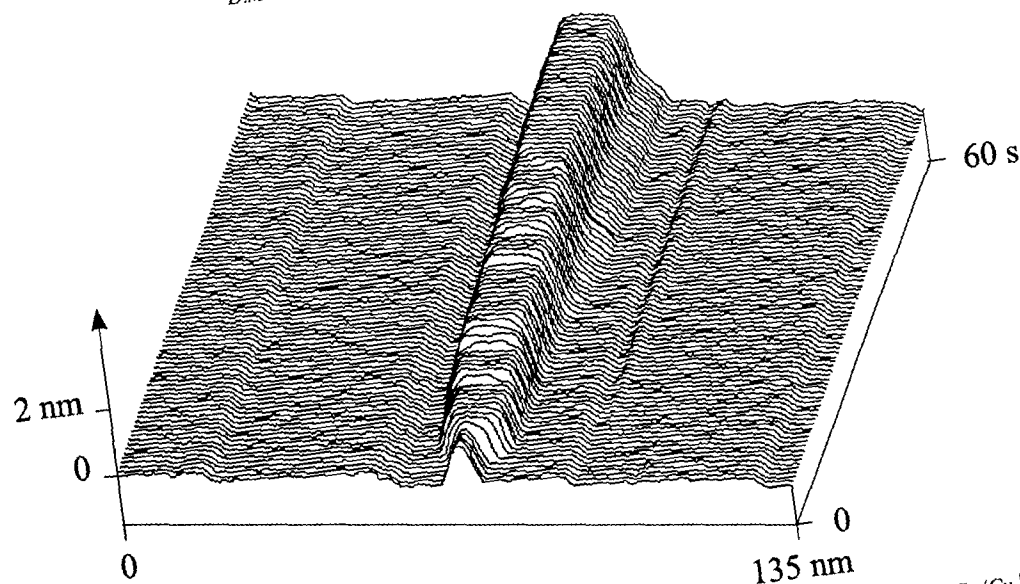
Fig. 4. STM image ($x - t$-scan) of a growing Cu cluster after stepping the potential from $+10$ mV to -280 mV vs. Cu/Cu^{++} (at $t = 2.5$ s). $E_{tip} = -30$ mV, $I_t = 2$ nA. Electrolyte: 0.05 M H$_2$SO$_4$ + 0.1 mM CuSO$_4$.

3.3. Ag clusters on Au(111)

Ag deposition on Au(111) starts at underpotentials like in the case of Cu [29,30]. Hence, the jump-to-contact occurs between bulk Ag on the tip and a Ag monolayer on Au(111), and the tip-generated Ag clusters are placed on the upd layer of Ag on Au(111). The successful decoration with Ag nano-clusters of a Au(111) electrode at $+0.1$ V vs. Ag/Ag$^+$, where the surface is covered by a mono-layer of Ag [30], is demonstrated in Fig. 6, which shows the STM image of a square array of 25 Ag clusters. A series of experiments has revealed that the reproducibility of the cluster generation process is by far not as good as for Cu on gold. This is particularly true for the cluster height which varies in Fig. 6 between 0.3 and 1.1 nm.

Like in the case of Cu on Au(111) [14,27], the Ag clusters are surprisingly stable against anodic disso-lution. Fig. 7 summarizes the results of a series of experiments, in which the heights of individual clusters were measured at certain time intervals for three different electrode potentials. We note that at a potential of $+50$ mV vs. Ag/Ag$^+$ the clusters are stable over several minutes and even for 'overpoten-tials' as high as 200 mV, the Ag clusters do not

dissolve momentarily. The reason for this unusually high stability was explained in a recent publication [27].

3.4. The Ni/Au(111) system

In an attempt to decorate a gold surface with nanoclusters of a magnetic metal, Ni was deposited onto the Pt/Ir tip in a so-called Watts bath. The latter is a commonly used electrolyte for Ni plating. However, after various externally enforced ap-proaches of the Ni-coated STM tip only holes in the Au(111) surface were seen, but no Ni clusters (Fig. 8a). This observation is in full agreement with the theoretical predictions of Landman et al. [23,24], who performed calculations for the interaction be-tween a Ni tip and a Au surface, and found a jump-to-contact from the gold to the nickel. This is schematically shown in Fig. 8c, illustrating the hole formation in the gold surface due to gold atoms jumping to the tip.

The STM image in Fig. 8a reveals that the hole production is rather erratic and works only a few times, since the tip was approached 25 times towards the surface. This may be explained by the fact that with the first jump-to-contact the Ni tip is trans-
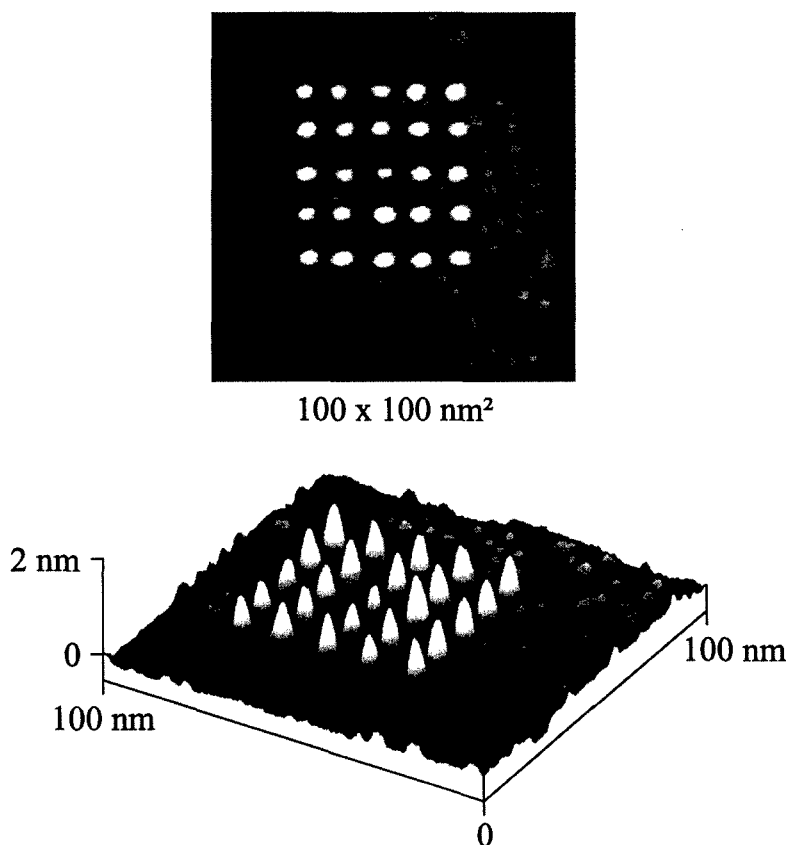
100 x 100 nm²

Fig. 5. STM image (top view and 3D-plot) of 25 Cu clusters placed on an ethanethiol-modified Au(111) surface in 0.05 M H_2SO_4 + 1 mM $CuSO_4$. E_{sample} = + 10 mV vs. Cu/Cu^{++}, E_{tip} = − 30 mV, I_t = 2 nA.
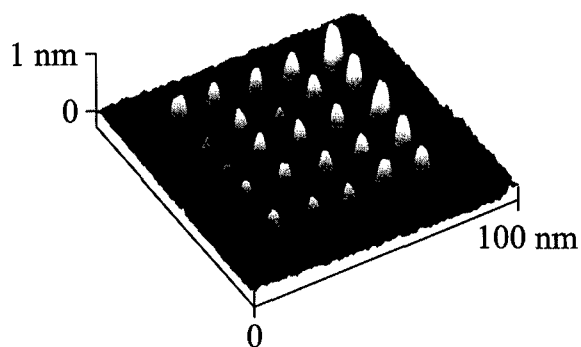

Fig. 6. STM image of 25 Ag clusters on Au(111) in 0.05 M H_2SO_4 + 0.1 mM Ag_2SO_4. E_{sample} = + 100 mV vs. Ag/Ag^+, E_{tip} = 0 mV, I_t = 2 nA.
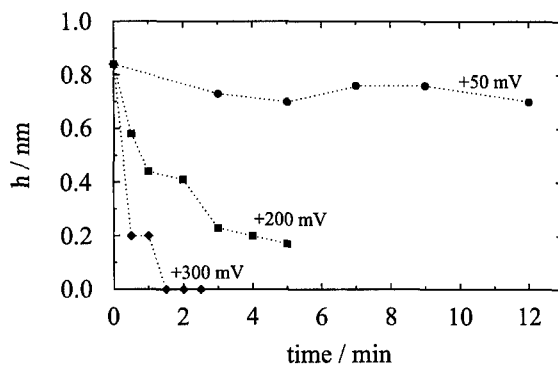

Fig. 7. Variation of cluster height with time during the dissolution of Ag clusters on Au(111) at various electrode potentials.
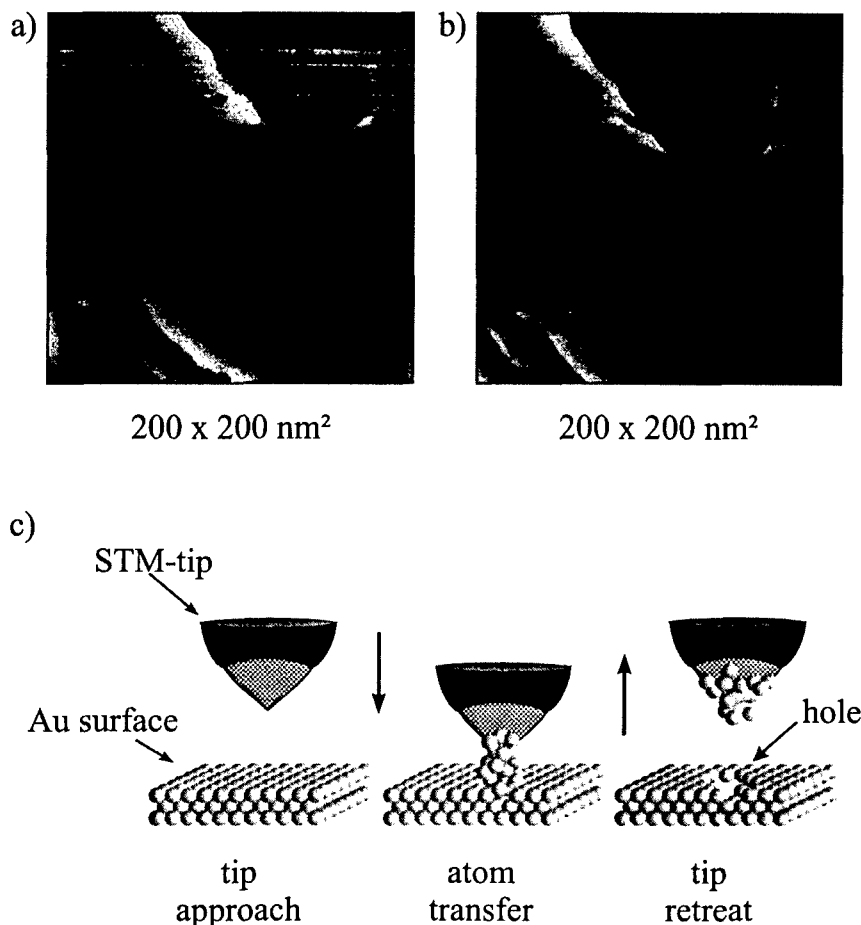
Fig. 8. (a) STM image of a Au(111) electrode in 1 mM $NiSO_4$ + 10 mM H_3BO_3 + 0.2 mM HCl, showing the hole formation with a Ni-covered Pt–Ir tip. The five lines in the upper part of the image reflect the pulses on the z-piezo (five pulses per line). E_{sample} = – 320 mV vs. SCE, E_{tip} = – 470 mV, I_t = 2 nA. (b) Same area, imaged 1 min later. E_{sample} = – 320 mV vs. SCE, E_{tip} = – 470 mV, I_t = 2 nA. (c) Suggested mechanism of the hole formation in the Au(111) substrate during the approach of a Ni-covered STM tip.

formed into a gold-covered tip. The image in Fig. 8b was recorded 1 min after the hole production and after image (a) and it demonstrates the relatively high mobility of the advacancy islands on gold which causes these holes to migrate to step edges or to merge with each other. We may briefly mention here, that preliminary experiments with Co^{++} containing electrolytes led to a tip-induced Co cluster formation on Au(111), although the production was very irregular. This system is currently under investigation.

3.5. Determination of tunnel barriers

The externally enforced tip approach for cluster fabrication can also be employed to determine rather precisely tunnel barriers at the metal–electrolyte interface. This has been demonstrated for Cu and Au(111) [26], where a barrier height of Φ_T = 1.5 eV was found. In Fig. 9 the logarithmic dependence of the momentarily flowing tunnel current I_T as a function of the tip approach Δz is shown. The latter can be converted from mV to nm by the conversion
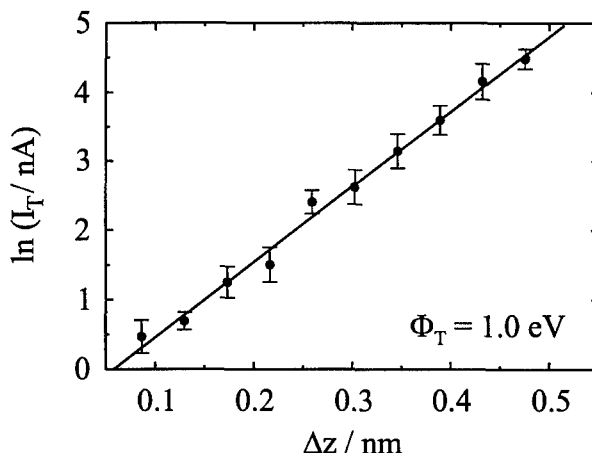
Fig. 9. Determination of the tunnel barrier height Φ_T from measurements of the tunnel current I_t as a function of the tip approach Δz, which was externally enforced by applying a voltage pulse to the z-piezo. Each data point is the average of five pulses. The error bars represent the S.D. for these five pulses.

factor given for this instrument by the manufacturer. During this type of measurement, the feed-back circuit of the STM is almost completely switched off (integral and proportional gain were 0.03 and 0, respectively, as compared to 1.5 and 2.0 for typical imaging conditions). The data points in Fig. 9 were obtained by applying voltage pulses of various heights and 20 ms duration onto the z-piezo. Plotting the height of the resulting tunnel current as a function of distance change Δz for each tip approach, yields an exponential dependence over a wide range. From the slope of the straight line in Fig. 9, a tunnel barrier of 1.0 ± 0.2 eV was determined for tunnelling from the tip to the substrate in 0.05 M H_2SO_4 + 1 mM Ag_2SO_4. The potential of the Au(111) substrate was held at $+ 0.25$ V vs. Ag/Ag$^+$, that of the tip at $+ 100$ mV vs. Ag/Ag$^+$. Under such conditions the Au(111) surface is covered by a monolayer of Ag [30].

Although the literature data for tunnel barriers in metal electrode–aqueous solution systems scatter widely, the values ranging from 0.2 [31,32] up to 3.8 eV [33], there seems to be a general agreement that the more recently published data which all jump between 1.0 and 1.5 eV [34,35], seem to be the most reliable ones. Hence, both values for the tunnel barrier determined by our method, 1.5 eV [26] for Cu

and 1.0 eV in the case of Ag, appear to be in the correct range of data.

Acknowledgements

References

[1] D.M. Eigler, E.K. Schweizer, Nature 344 (1990) 524.
[2] M.T. Cuberes, R.R. Schlitter, J.K. Gimzewski, Surf. Sci. 371 (1997) L231.
[3] Ph. Avouris, J.-W. Lyo, Appl. Surf. Sci. 60–61 (1992) 426.
[4] G. Meyer, S. Zöphel, K.H. Rieder, Appl. Phys. A 63 (1996) 557.
[5] C. Thirstrup, M. Sakurai, T. Nakayama, M. Aono, Surf. Sci. 411 (1998) 203.
[6] M.F. Crommie, C.P. Lutz, D.M. Eigler, Science 262 (1992) 218.
[7] W. Li, J.A. Virtanen, R.M. Penner, Appl. Phys. Lett. 60 (1992) 1181.
[8] W. Li, J.A. Virtanen, R.M. Penner, J. Phys. Chem. 96 (1992) 6529.

[9] X.H. Xia, R. Schuster, V. Kirchner, G. Ertl, J. Electroanal. Chem. 461 (1999) 102.

[10] D. Hofmann, W. Schindler, J. Kirschner, Appl. Phys. Lett. 73 (1998) 3279.

[11] R.T. Pötzschke, G. Staikov, W.J. Lorenz, W. Wiesbeck, J. Electrochem. Soc. 146 (1999) 141.

[12] R. Ullmann, T. Will, D.M. Kolb, Chem. Phys. Lett. 209 (1993) 238.

[13] D.M. Kolb, R. Ullmann, T. Will, Science 275 (1997) 1097.

[14] D.M. Kolb, R. Ullmann, J.C. Ziegler, Electrochim. Acta 43 (1998) 2751.

[15] G.E. Engelmann, J.C. Ziegler, D.M. Kolb, J. Electrochem. Soc. 145 (1998) L33.

[16] J.C. Ziegler, G.E. Engelmann, D.M. Kolb, Z. Phys. Chem. 208 (1999) 151.

[17] J. Wiechers, T. Twomey, D.M. Kolb, R.J. Behm, J. Electroanal. Chem. 248 (1988) 451.

[18] L.A. Nagahara, T. Thundat, S.M. Lindsay, Rev. Sci. Instrum. 60 (1989) 3128.

[19] C.E. Bach, R.J. Nichols, W. Beckmann, H. Meyer, A. Schulze, J.O. Besenhard, P.D. Jannakoudakis, J. Electrochem. Soc. 140 (1993) 1281.

[20] T. Will, M. Dietterle, D.M. Kolb, in: A.A. Gewirth, H. Siegenthaler (Eds.), Nanoscale Probes of the Solid–liquid Interface, NATO ASI, Vol. E 288, Kluwer, Dordrecht, 1995, p. 137.

[21] J. Clavilier, R. Faure, G. Guinet, R. Durand, J. Electroanal. Chem. 107 (1980) 205.

[22] H. Hagenström, M.A. Schneeweiß, D.M. Kolb, Langmuir 15 (1999) 7802.

[23] U. Landman, W.D. Luedtke, N.A. Burnham, R.J. Colton, Science 248 (1990) 454.

[24] U. Landman, W.D. Luedtke, in: R. Wiesendanger, H.-J. Güntherodt (Eds.), Scanning Tunnelling Microscopy III, Springer Series in Surface Science, Vol. 29, Springer, Berlin, 1993, p. 207.

[25] R. Ullmann, Ph.D. thesis, University of Ulm, 1997.

[26] G.E. Engelmann, J.C. Ziegler, D.M. Kolb, Surf. Sci. 401 (1998) L420.

[27] D.M. Kolb, G.E. Engelmann, J.C. Ziegler, Angew Chem. Int. Ed. 39 (2000) 1123; Angew Chem. 112 (2000) 1166.

[28] G.E. Engelmann, D.M. Kolb, to be published.

[29] K. Ogaki, K. Itaya, Electrochim. Acta 40 (1995) 1249.

[30] M.J. Esplandiu, M.A. Schneeweiß, D.M. Kolb, Phys. Chem. Chem. Phys. 1 (1999) 4847.

[31] M. Binggeli, D. Carnal, R. Nyffenegger, H. Siegenthaler, R. Christoph, H. Rohrer, J. Vac. Sci. Technol. B9 (1991) 1985.

[32] J. Halbritter, G. Repphun, S. Vinzelberg, G. Staikov, W.J. Lorenz, Electrochim. Acta 40 (1995) 1385.

[33] J. Pan, T.W. Jing, S.M. Lindsay, J. Phys. Chem. 98 (1993) 4205.

[34] S. Vinzelberg, Ph.D. thesis, University of Karlsruhe, 1995.

[35] A. Vaught, T.W. Jing, S.M. Lindsay, Chem. Phys. Lett. 236 (1995) 306.